Petroleum Science 23 (2026) 1955–1969

Contents lists available at ScienceDirect

Petroleum Science

journal homepage: www.keaipublishing.com/en/journals/petroleum-science

Original Paper

A high-temperature and high-strength polymer gel for plugging in fractured formations

Yuan Liu [a], Ying-Rui Bai [a,*], Jin-Sheng Sun [a,b], Kai-He Lv [a], Jing-Bin Yang [a], Ke-Qing Yang [a], You-Ming Lang [a]

[a] School of Petroleum Engineering, China University of Petroleum (East China), Qingdao, 266580, Shandong, China
[b] CNPC Engineering Technology R&D Company Limited, Beijing, 102206, China

ARTICLE INFO

Article history:
Received 11 May 2025
Received in revised form
4 January 2026
Accepted 4 January 2026
Available online 7 January 2026

Edited by Jia-Jia Fei

Keywords:
Polymer gel
Plugging
Fracture
Temperature
Mechanical properties

ABSTRACT

Lost circulation, the significant penetration of drilling fluid into formations during drilling, leads to excessive fluid consumption, non-productive time, and potential well control incidents. This study developed a tunable polymer gel system for plugging lost circulation zones of various scales. Its mechanical properties can be controlled by adjusting the concentration, temperature, gelling time, and aging time. At 120 °C and 10 h gelling time, increasing concentration from 12% to 20% steadily enhanced mechanical properties: storage modulus rose from 750 to 3171 Pa, and tensile stress increased from 20.03 to 67.8 kPa. However, under different temperature and time regimes, the mechanical properties of polymer gels first strengthened and then weakened or showed a trend of strengthening, weakening, and then strengthening again. For example, under gelling temperature 120 °C and 14% concentration, when the gelling time was increased from 4 to 10 h, the tensile stress of polymer gel increased from 4.103 to 30.07 kPa, but when the gelling time was further extended from 10 to 12 h, the tensile stress was reduced from 30.07 to 11.33 kPa. With further extension of time to 14 h, the tensile stress increased again to 43.91 kPa. Comprehensive microstructural analysis revealed how these factors influence gel properties. Subsequently, the simulated plugging experiments of fractures and sand-filled pipes were conducted using the polymer gel with a concentration of 14% and a temperature of 140 °C for 8 h, and the plugging strength was 5.8 MPa for the parallel fracture of 5 mm, and 10.06 MPa for the sand-filled pipe with a 3 mm fracture and an inner diameter of 3 cm in the outlet pipe, which indicated that the polymer gel system exhibited strong pressure-bearing plugging ability for both the fracture and the fracture/vuggy. The proposed polymer gel was applied in the field of HD29-H8 well in the Tarim Basin of Xinjiang, China, and successfully plugged the loss formation above 5000 m, which demonstrated that it can effectively plug high-temperature and high-pressure reservoirs.

1. Introduction

Polymer gel is a gel system composed of polymer substances, characterized by a three-dimensional crosslinking network formed through physical or chemical crosslinking. Physical crosslinking relies on non-covalent interactions such as hydrophobic associations, hydrogen bonding, electrostatic forces, and van der Waals forces. Gels formed by these reversible interactions have weaker strength but allow dynamic sol-gel transitions. In contrast, chemically crosslinked gels exhibit stronger structural stability and mechanical strength but lower degradability, raising environmental concerns. Compared with conventional gels, polymer gels display structural discontinuities that provide higher deformability, faster environmental responsiveness, and strong viscoelasticity (Bai et al., 2023). They also possess high porosity, reversible deformability, and excellent water absorption (Kwon et al., 2023). With oil and gas exploration expanding into deep, ultra-deep, and unconventional reservoirs, operational environments have become increasingly harsh. Due to their mechanical deformability, polymer gels can penetrate loss channels of varying sizes, resist dilution by formation water or drilling fluid, and form high-strength plugs in fractures. Thus, they are widely used in loss

* Corresponding author.
E-mail address: smart-byron@163.com (Y.-R. Bai).
Peer review under the responsibility of China University of Petroleum (Beijing).

https://doi.org/10.1016/j.petsci.2026.01.001

prevention, plugging, fracturing, cementing, profile control, water shutoff, and enhanced recovery (Pu et al., 2018; Sun et al., 2023; Zou et al., 2023). Existing polymer gel plugging materials mainly include underground crosslinking, ground pre-crosslinking, and non-crosslinking types, each with specific advantages and conditions (Bai et al., 2015a). For fractured formations, conventional bridging materials such as walnut shells, calcite, and rubber often suffer from size mismatch (Elahifar et al., 2023; Sun et al., 2019). Traditional guar and xanthan gum gels show low mechanical strength and poor thermal stability (Yang et al., 2024; Zhu et al., 2021), resulting in reduced plugging efficiency and higher operational costs. In contrast, polymer gels have controllable gelling time, high adaptability to fracture sizes, and tunable mechanical properties under various conditions (Feng et al., 2017; Xiong et al., 2018; Vargas et al., 2020; Yun et al., 2021).

Characterizing the rheology and stress-strain behavior of polymer gels is essential for evaluating their mechanical properties. Academician Luo Pingya proposed that gel rheology in fractures should have seven characteristics, "flowing into, not diluting, stopping, discharging, filling, isolation, and resistance" (Wang et al., 2012). Recent studies have focused on optimizing gel structure and formulation to improve mechanical performance (Zhang et al., 2017; Bai et al., 2022). In addition, higher polymer concentration increases viscosity, while temperature changes may rearrange the gel structure and break crosslinking points. Greater crosslinking degrees enhance network density and connection strength (An et al., 2016; Cao et al., 2017; El et al., 2023; Ma et al., 2024). Furthermore, the type of rheological modifier and solid particle size distribution significantly influence gel rheology and mechanics (Azimi et al., 2019; Smilek et al., 2019). For the high temperature stability of polymer gels, Qiu Zhengsong's team (Chen et al., 2018) prepared a high acid-soluble fiber plugging agent resistant up to 150 °C, which improved fracture plugging when combined with other materials. Higher apparent viscosity and viscoelasticity enhance a gel's resistance to dissolution by drilling fluids or formation water, maintaining integrity within fractures, though reduced fluidity may hinder injection. To address this, researchers examined the relationship between apparent viscosity, elastic modulus, and time variation to determine optimal injection timing and predict gel strength (Lu et al., 2015; Dai et al., 2017). A polymer gel synthesized through hydrophobic bonding showed strong ductility and excellent linear viscoelasticity below 10% strain, with a tensile stress of 2.33 MPa at 300% elongation (Du et al., 2023). To address issues of short gelling time, weak strength, and poor stability, Bai et al. (2018) synthesized a high-strength, weakly thixotropic plugging agent using aluminum-magnesium layered double hydroxide and modified clay for medium-low temperature fractured zones. Xie et al. (2021) found that optimized polymer concentration yielded shear strength of 5000 Pa, and at 140 °C, the gel maintained high elasticity and gel strength. According to crosslinking methods, the tensile modulus of polymer gels varies in the order of covalently bonded, non-covalently bonded, and hybrid crosslinked gels (Liao et al., 2018). For non-covalent gels, higher synthesis temperature reduces effective crosslinking sites, weakening tensile performance and increasing elongation at break (Jiang et al., 2014).

Scholars worldwide have also investigated polymer gel mechanisms in loss prevention, profile control, flooding, and water shutoff. Polymer microspheres with small, uniform particles and good dispersibility have been synthesized to achieve temporary plugging through multi-particle bridging, thereby improving deep formation flow regulation (Yao et al., 2015; Zhao et al., 2019; Lin et al., 2022). Regarding the mechanism of profile control, water shutoff, and loss prevention, Ivan et al. (2002) proposed that crosslinked polymer bridge plugs create robust pressure-bearing barriers within fractures, isolating low-pressure formations from high-pressure wellbores by halting fracture propagation. Sweatman et al. (2004) demonstrated that the gel slug in formation fractures causes a pressure drop from the wellbore to the formation, reducing the pressure at the fracture tip and preventing further expansion. Therefore, strengthening gel internal strength and its adhesion with fracture walls is crucial to increasing the pressure-bearing window. Bai et al. (2015b) found that successful plugging requires the sum of gel cohesion and viscous adhesion to exceed the pressure differential across the fracture; thus, enhancing adhesion between the gel and fracture wall is key to effective plugging.

Current research primarily focuses on developing new polymer gel systems and improving properties by modifying raw materials, optimizing formulations, or changing crosslinking methods. However, systematic studies on the combined effects of concentration, temperature, gelling time, and aging on mechanical properties remain limited. This study therefore investigates these factors by preparing gels under varied conditions, performing rheological and mechanical tests, and analyzing corresponding microstructural and morphological changes. Through laboratory fracture core and sand-filled pipe plugging experiments, as well as field evaluations, this work aims to clarify the mechanisms influencing gel mechanical behavior and provide insights for optimizing polymer gel performance under complex reservoir conditions.

2. Experiment

2.1. Experimental materials

The chemicals used to synthesize the polymer gel included polyacrylamide (PAM, 99.0%, Shanghai McLean Biochemical Technology Co., Ltd.), N-methylacrylamide (NMA, 98.0%, Shanghai McLean Biochemical Technology Co., Ltd.), tert-butyl hydroperoxide (TBHP, 70% aqueous solution, Shanghai McLean Biochemical Technology Co., Ltd.), urea-formaldehyde resin (AR, Jinan Dahui Chemical Technology Co., Ltd.), silicate fiber (Hebei Teyan Gold Trading Co., Ltd.), lithium-based bentonite (98%, Bayer, Germany), and deionized water was homemade in the laboratory.

2.2. Characterization of polymer gel properties

2.2.1. Infrared characterization

The polymer gel's chemical structure was examined using a Fourier transform infrared spectrometer (model: IRTRacer-100; SHIMADZU Corporation, Japan). Before testing, the polymer gel was washed with deionized water to eliminate unreacted materials, then dried in a vacuum oven and ground into powder. Samples were made using the potassium bromide compression method. The infrared wavelength scanning range is 4000–500 cm^{-1} with 4 cm^{-1} resolution and 50 times scans.

2.2.2. Microscopic morphology test

To obtain the microstructure of the polymer gel, the microstructure was characterized using a scanning electron microscope (SEM; model Apreo 2S; THERMOFISHER, Germany). To prepare a freeze-dried polymer gel, the samples were first frozen in liquid nitrogen and dried for 48 h at −50 °C and 30 × 10^{-3} mbar of pressure. Then the samples were fixed on the test platform with conductive tape, and gold powder was coated on the surface to enhance conductivity. Finally, the samples were put into the SEM sample chamber to obtain microscopic images with different magnifications at room temperature. To more clearly analyze the influence of changes in component concentration, temperature,

gelling time and aging time on the microstructure, this study selected the same scale for comparison in the microstructure analysis of each influencing factor.

2.2.3. Rheological mechanical property test

A high-temperature and high-pressure rotational rheometer (model: HAAKE MARS 60; Thermo Fisher Scientific, Germany) was used for the test. A P35/Ti flat rotor with a 35 mm diameter was used in the experiment. The strain scanning test was conducted on the gel sample, with a fixed shear frequency of 1 Hz and a testing temperature of 20 °C. The changes in the storage modulus (G') and loss modulus (G'') of the samples were tested in the strain range of 0.1%–1000%. The gel sample underwent an angular frequency scanning test, with the shear strain fixed at 1% and the test temperature at 20 °C. The changes in the storage modulus (G') and loss modulus (G'') of the samples were tested in the range of angular frequency from 0.1 to 100 rad/s.

2.2.4. Mechanical property test

The electronic universal testing machine (model: CMT4000; The New Sans Material Testing Company, Shenzhen, China) was used to conduct uniaxial tensile mechanical property testing on the polymer gels at room temperature. The laboratory environmental humidity is 40%. The gels were made into a dumbbell form and coated with a thin layer of silicone oil to prevent moisture loss during stretching, which could cause inaccurate test data. The tensile rate was set at 50 mm/min, and the stress-strain curves were recorded for the samples.

2.2.5. Test of polymer gel plugging performance

The gel's plugging ability was tested with a high-temperature, high-pressure fracture simulation device (Nantong Xinhua Cheng Scientific Instruments Co., Ltd., Nantong, China) (Fig. 1). We synthesized a polymer gel solution with 14% concentration, stirred well and poured into the high-temperature and high-pressure plugging instrument. The solution was injected into the vertical fractures and filled the fracture space. Then the temperature was increased to 140 °C, and after 8 h of gelling, the pressure-bearing plugging strength on the fracture was tested. In this experiment, parallel steel fracture with an inlet and outlet size of 20 mm × 5 mm was used to simulate microfractures induced by formation stress, while sand-filled steel pipes with an inlet and outlet line of 3 mm, an inner diameter of 3 cm and a length of 20 cm simulated the plugging performance for loss-off scenarios through fractures connecting vuggy.

3. Preparation of polymer gel

3.1. Preparation method of polymer gel

The polymer gel was prepared through the following steps: (a) weighing a certain amount of polyacrylamide and N-hydroxymethacrylamide poured into deionized water, followed by continuous stirring to ensure complete and uniform dissolution of the polymer powder; (b) a specified amount of lithium-based bentonite and urea-formaldehyde resin was added to the polymer solution from step (a), followed by continuous stirring to ensure uniform dispersion and dissolution of both components; (c) a measured amount of silicate fiber was slowly added to the solution from step (b), with continuous stirring to achieve uniform dispersion; (d) a specified amount of tert-butyl peroxide initiator was then introduced into the mixture from step (c), followed by constant stirring to ensure full dissolution and mixing. The solution was stirred until it reached a thick, uniform state without phase separation, forming the polymer gel system. The component contents of the polymer gel system are shown in Table 1.

The prepared polymer gel system with concentrations of 12%, 14%, 16%, 18%, and 20% were heated in a roller furnace at 80, 100, 120, and 140 °C for 2, 4, 8, 10, 12, and 14 h to obtain polymer gels. From the perspective of physical structure, the gel system of high molecular polymer can form a solidified product with a certain toughness and three-dimensional network structure after gelling. Fig. 2(a) shows the process of acrylamide polymerization to generate high molecular polymer. For low concentration, low gelling temperature, and short gelling time, the polymer gel system remains in a dilute state. During the gelling process, the

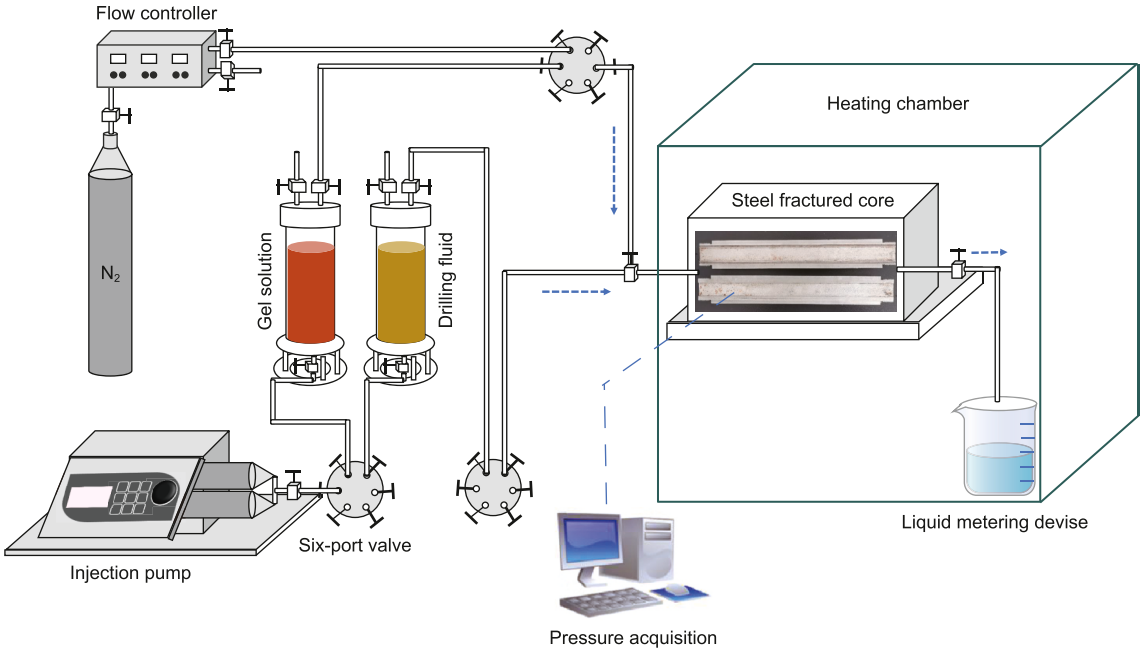

Fig. 1. High-temperature and high-pressure fracture plugging simulation device.

Table 1
Component content of polymer gel system.

Material	PAM	NM	Urea-formaldehyde resin	Lithium-based bentonite	Silicate fibers	TNHP
Mass percentage, wt%	15	0.6	0.5	2.5	1.5	0.01

* Deionized water was added based on the concentration of the polymer gel system.
* The following experiments and field applications were all conducted using this formulation.

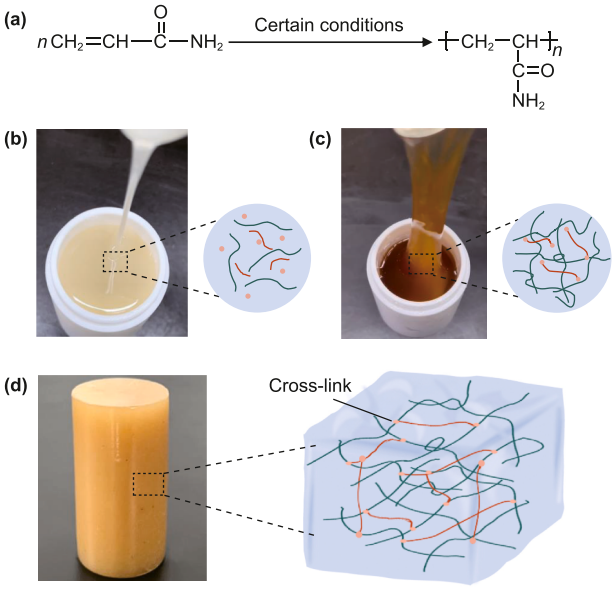

Fig. 2. (**a**) Chemical equation for polymerization reaction of acrylamide to produce polymer; (**b**) schematic microstructure of dilute solution before gelling; (**c**) schematic microstructure during the gelling process; (**d**) schematic microstructure of the gel after gelling.

individual molecular chains are separated and do not overlap, resulting in a dilute solution as shown in Fig. 2(b) (Kumaki et al., 2015). With the increase of concentration, gelling temperature, gelling time, thermodynamics and other physical properties of the system change significantly. Molecular chains begin to cross, overlap and entangle with each other, forming a tangled network with a uniform distribution of chain segments as shown in Fig. 2(c) (Zhao et al., 2013). When the concentration, gelling temperature and gelling time are sufficiently high, the molecular chains of the polymer overlap and entangle extensively, forming a three-dimensional crosslinking network structure as shown in Fig. 2(d), which results in a macroscopic transition from viscous flow to elastic state. The polymer solution thus loses its fluidity and forms a polymer gel (Son et al., 2022).

3.2. Polymer gel infrared spectroscopy analysis

To analyze the molecular structure, the Fourier transform infrared spectrum is shown in Fig. 3. The absorption peaks at 3183, 2953, 2831, 1600, 1363, 1113, and 774 cm^{-1} are very noticeable. The amino N–H stretching vibration is responsible for the broad absorption peak at 3183 cm^{-1}; the C–H stretching vibration absorption peaks are at 2953 and 2831 cm^{-1}; the C=O stretching vibration absorption peak is at 1600 cm^{-1}; the C–N stretching vibration absorption peak is at 1363 cm^{-1}; the NH_2 plane vibration peak of acrylamide polymerization into polyacrylamide is at 1113 cm^{-1}; and the C–H bond out-of-plane bending vibration is at 774 cm^{-1}. These absorption peaks are representative features of polyacrylamide gel, indicating that the target products of the polymer gel system were obtained after synthesis.

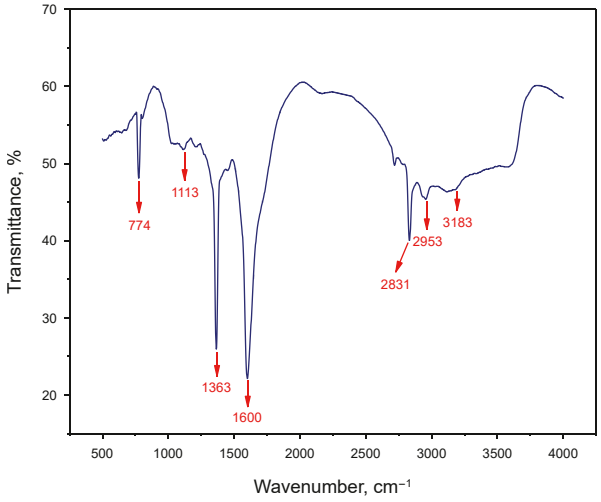

Fig. 3. Infrared spectrum of the polymer gel.

4. Effect of component concentration on gel properties

4.1. Effect on pheological mechanical properties

To investigate the impact of concentration on gel's rheological properties, the changes in storage modulus and loss modulus under strain and angular frequency changes were systematically investigated by adjusting the concentration of the polymer gels (12%–20%) under gelling temperature of 120 °C and gelling time of 10 h. As shown in Fig. 4(a), the storage modulus of polymer gel started to change at strain $\gamma = 100\%$, which decreased sharply. Therefore, the gel's linear viscoelastic region lay in the range of strain less than 100%, beyond which the polymer gel started to undergo gel phase transition. In the case of strain condition $\gamma = 10\%$, the polymer gel with concentration increased from 12% to 20%, its storage modulus rose from 43 to about 3171 Pa, and the loss modulus grew from 41 to about 285 Pa. To investigate how angular frequency influences the rheological behavior of polymer gels at varying concentrations, angular frequency scanning was conducted on different concentrations of polymer gel under constant strain $\gamma = 1\%$ (Fig. 4(b)). When the angular frequency was 0.1–1 rad/s, the storage modulus and loss modulus increased significantly, and then grew slowly. The overall increase in loss modulus was less than that of storage modulus. When the polymer gel concentration was increased from 12% to 20%, its storage modulus eventually stabilized at around 113 and 1582 Pa, and its loss modulus eventually stabilized at around 120 and 640 Pa. This indicates that the storage modulus of the polymer gel increases with angular frequency, demonstrating enhanced elasticity of its internal network structure. In combination with the physical images in Fig. 5(b–f), this reveals that as the concentration increased, the gelling effect of the gel became better, and the physical appearance of the polymer gel with a concentration of 20% was intuitively denser than that of the polymer gel with a concentration of 16%. According to the scanning electron microscope image analysis of Fig. 5(g) and (h), it was observed that the microstructure appeared less wrinkled and smoother. This is due to

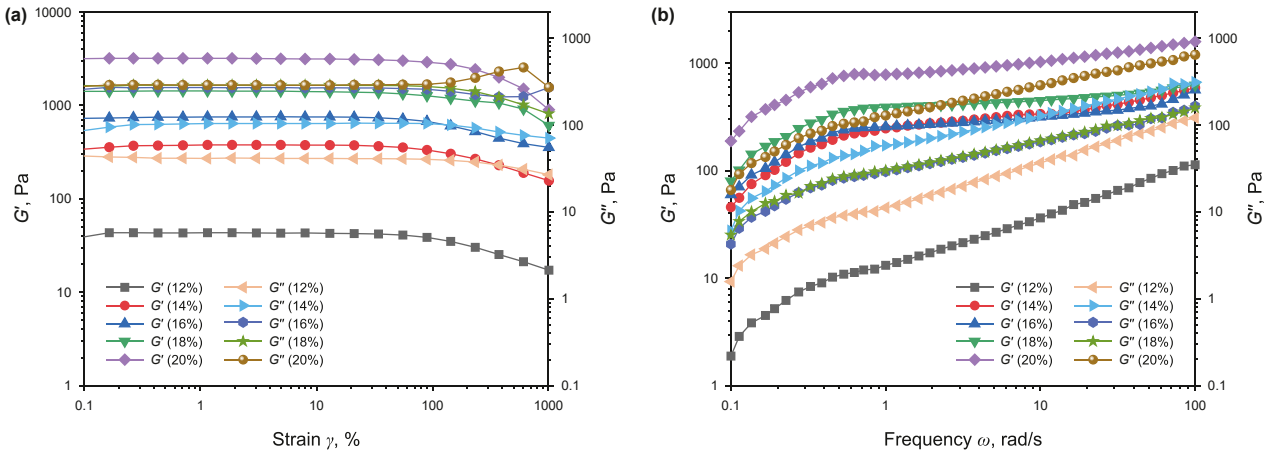

Fig. 4. Gelling temperature at 120 °C, gelling time of 10 h: (**a**) relationship between strain and modulus with different concentrations; (**b**) relationship between angular frequency and modulus with different concentrations.

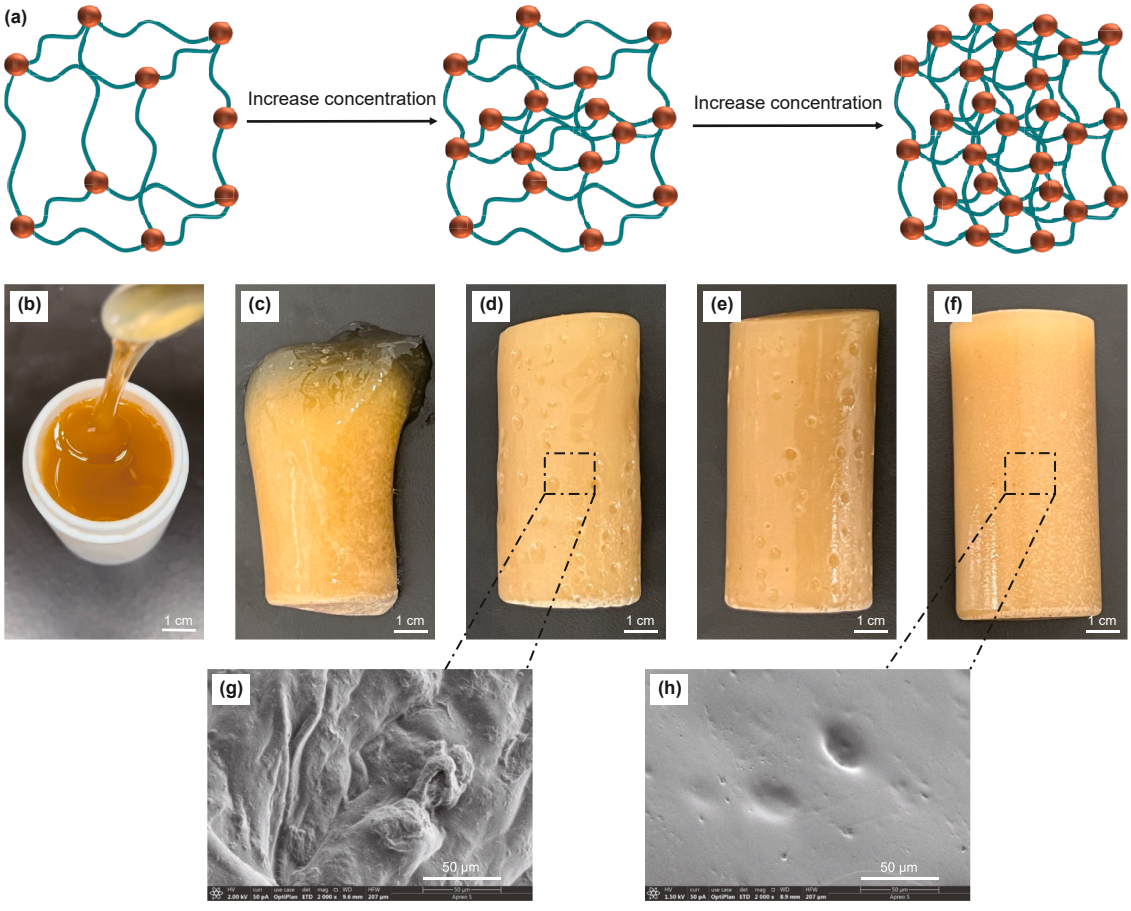

Fig. 5. (**a**) Schematic diagram of the internal network structure of polymer gels with different concentrations; (**b**–**f**) physical images of gels with different concentrations at a gelling temperature of 120 °C and a gelling time of 10 h: (**b**) 12%; (**c**) 14%; (**d**) 16%; (**e**) 18%; (**f**) 20%; (**g**–**h**) SEM images of gels with different concentrations at a gelling temperature of 120 °C and a gelling time of 10 h: (**g**) 16%; (**h**) 20%.

the increase of crosslinking points of molecular chains under high concentration conditions, forming a more compact crosslinking network structure as shown in Fig. 5(a), significantly enhancing the gel's energy storage capacity. Meanwhile, the nonlinear increase in loss modulus is due to the tight crosslinking of molecular chains with the increase in polymer gel concentration, and the enhancement of their interactions leads to the enhancement of friction loss inside the gel at high concentration.

4.2. Effect on mechanical properties

Adjusting the concentration altered the gel's deformation behavior (Fig. 6), directly impacting its tensile strength and elongation at break. Experimental results (Fig. 7) indicated that higher concentrations led to a marked increase in tensile strength, accompanied by a decrease in elongation at break. When the concentration was adjusted of the polymer gel from 12% to 20%,

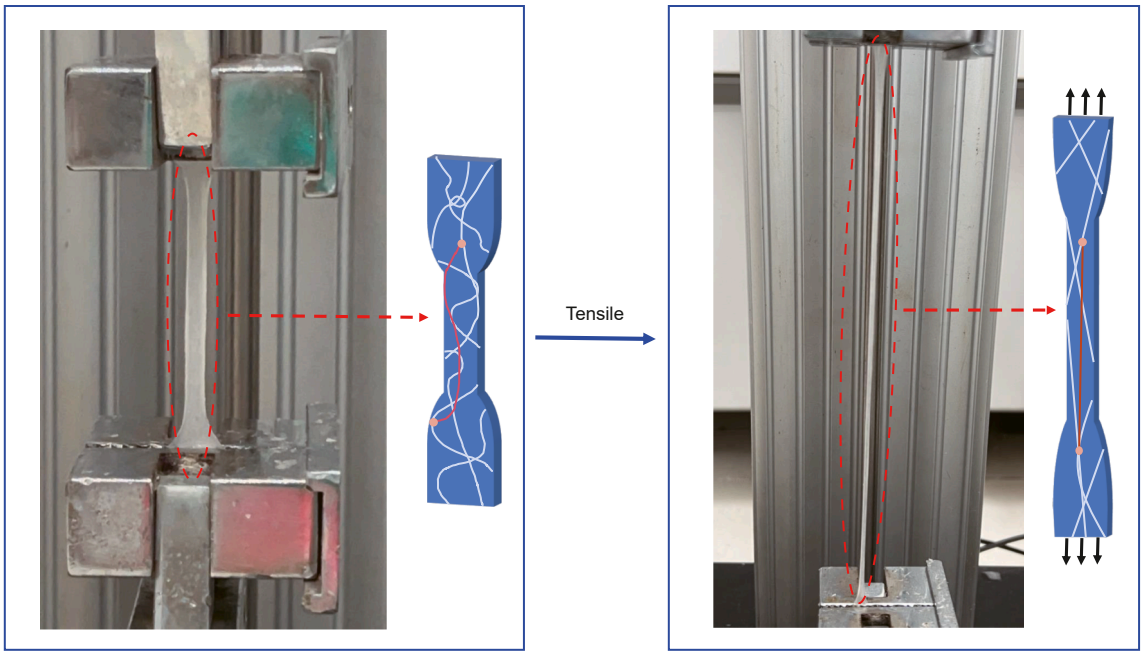

Fig. 6. Schematic diagram of structural changes of the gel before and after stretching.

the tensile stress of the polymer gel increased from 20.03 to 67.8 kPa, and the elongation at break decreased from 1003.93% to 240.28%. This variation was due to the polymer gel exhibited a higher storage modulus as the concentration increased, leading to the formation of more crosslinking points between molecular chains, effectively preventing the sliding and relative displacement of molecular chains, and constructing a denser network structure. This denser structure enhances the overall structural strength, causing the tensile stress of the polymer gel to increase with increasing concentration. However, as the concentration increased, the loss modulus also increased, the internal structure of the gel became more compact at high concentration, and the molecular chains were more densely crosslinked, which made it difficult to deform and stretch during tension, resulting in easier fracture as the stress increased. The polymer gel gradually exhibited brittleness, even though it performed well in strength, the deformation that occurred in the gel at the limit of the force was relatively small. Therefore, when designing and selecting polymer gels for oilfield field plugging, factors like the needed gel strength, fracture breadth, and depth must all be carefully taken into account. By adjusting the concentration of the polymer gel, its strength, ductility, and deformation ability can be altered to meet the requirements of specific field applications.

5. Effect of temperature on gel properties

5.1. Effect on rheological mechanical properties

As a key parameter for polymer gels preparation, the effect of gelling temperature on the rheological behavior of gels is of significant research value. Under the conditions of a gelling time of 10 h and a concentration of 14%, the storage modulus and loss modulus were found to exhibit a complex trend with increasing gelling temperature based on rheological experiments. When the temperature was raised from 80 to 100 °C under a strain condition of $\gamma = 10\%$, the polymer gel's storage modulus increased from around 0.9 to 870 Pa and its loss modulus increased from 1.93 to 525 Pa. When the temperature was further rose from 100 to 140 °C, the storage modulus decreased to around 335 Pa, and the loss modulus decreased to about 102 Pa. These data show that the storage modulus and loss modulus were the smallest from 0.1% to 1000% strain at 80 °C. However, when the gelling temperature increased to 100 °C, although both the storage modulus and loss modulus reached maximum, the gel could not maintain stable performance under external strain conditions, suggesting an unsatisfactory gelling effect at that temperature (Fig. 9(b)). As the gelling temperature increased to 120 °C, the storage modulus and loss modulus gradually exhibited better elasticity. However, when the gelling temperature increased to 140 °C, the storage modulus decreased slightly, while the loss modulus remained comparable to that at 120 °C. This suggests that in the range from 120 to 140 °C, the elasticity of the polymer gel decreased, and its rheological properties began to deteriorate (Fig. 8(a)). As shown in Fig. 8(b), angular

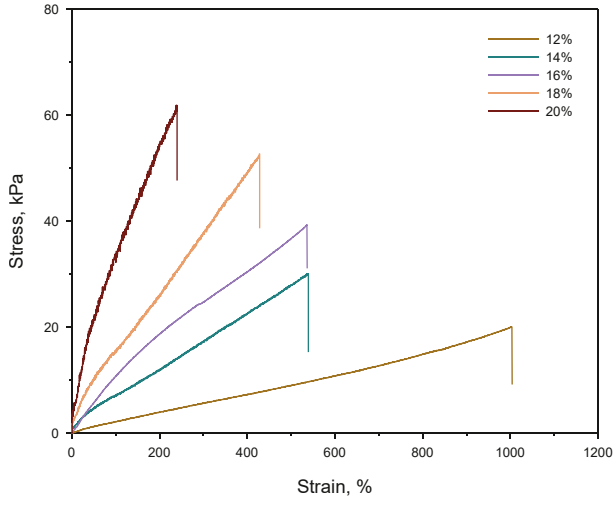

Fig. 7. Relationship between tensile stress and strain of gels with different concentrations at a gelling temperature of 120 °C and a gelling time of 10 h.

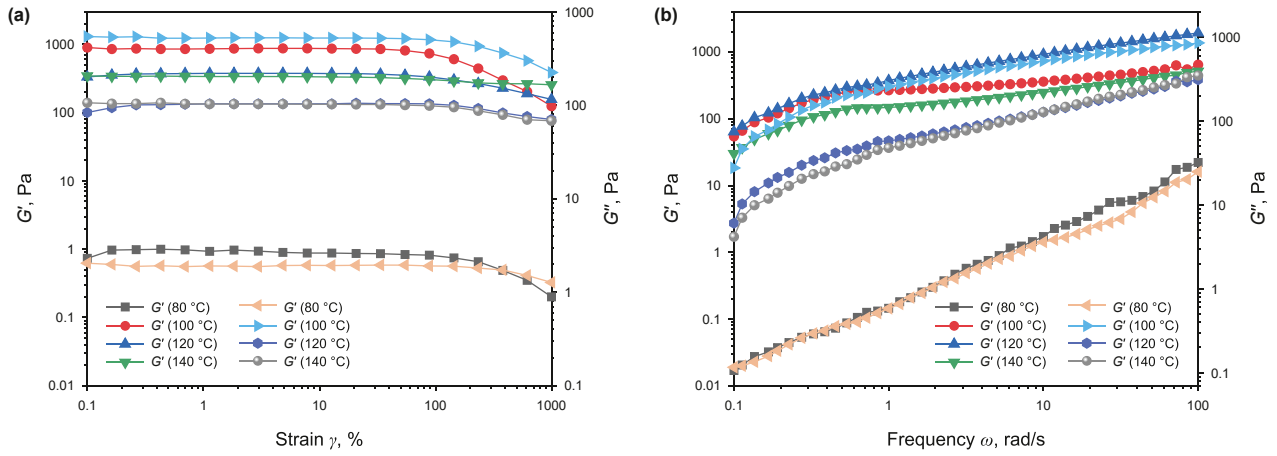

Fig. 8. Gelling time 10 h, 14% concentration: (**a**) relationship between gel strain and modulus at different gelling temperatures; (**b**) relationship between gel angular frequency and modulus at different gelling temperatures.

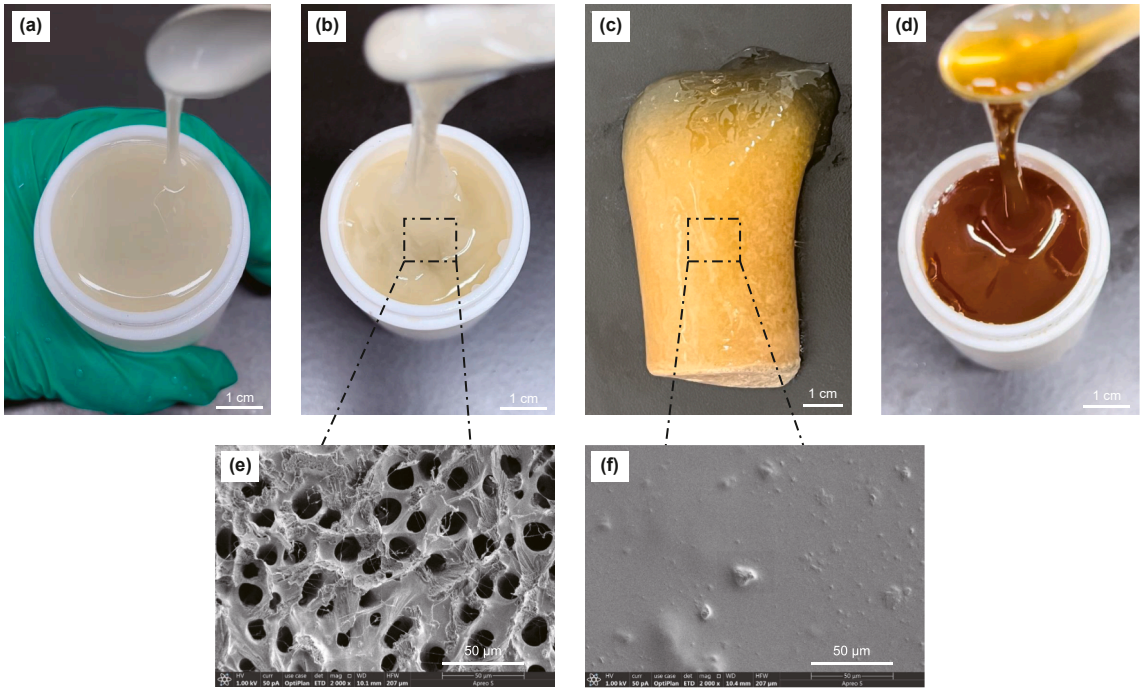

Fig. 9. (**a**–**d**) Physical images of gel formed at different gelling temperatures with a gelling time of 10 h and a concentration of 14%: (**a**) 80 °C; (**b**) 100 °C; (**c**) 120 °C; and (**d**) 140 °C; (**e**, **f**) gelling time 10 h, 14% concentration, SEM images of different gelling temperatures: (**e**) 80 °C; (**f**) 120 °C.

frequency scanning of gels prepared at different gelling temperatures was performed at a constant strain of $\gamma = 1\%$. At angular frequencies ranging from 0.1 to 100 rad/s, when the gelling temperature of the polymer gel was increased from 80 to 140 °C, the storage modulus eventually stabilized at around 22 and 646 Pa, and the loss modulus stabilized at about 25 and 348 Pa. Both storage modulus and loss modulus increased initially and then decreased with increasing gelling temperature. When the gelling temperature was 120 °C, the storage modulus reached its maximum, stabilizing at 1927 Pa, while the loss modulus remained relatively low, stabilizing at 310 Pa. These findings demonstrate that the gelling temperature significantly affects polymer chain arrangement and the degree of crosslinking. At low gelling temperatures, polymer chains tend to form disordered structures, and the resulting pore surfaces are rough, leading to poor viscoelasticity (Fig. 9(e)). At higher gelling temperatures, the gel exhibits no honeycomb, pits, wrinkles, or other morphologies, and its microstructure is smoother and denser (Fig. 9(f)). This results from the temperature rise, which enhances the degree of crosslinking, making the chain arrangement more orderly and forming a denser structure, effectively improving the viscoelasticity of the gel. However, excessive temperature may cause water loss and hardening of the gel due to combined thermal and shear effects, resulting in decreased elasticity. This demonstrates that the gelling temperature plays a significant role in regulating the internal microstructure of the gel. In the context of the experimental polymer gel system, the gel prepared at a gelling temperature of 120 °C exhibits the highest storage modulus and the smallest loss modulus, with the best gelling effect, so it has a better

stability under the long-time shear in the process of well loss plugging, which is of practical significance for the application in the field of well loss plugging.

5.2. Effect on mechanical properties

At low gelling temperatures, such as 80 and 100 °C, the polymer gel exhibited a low crosslinking density, and the storage modulus and loss modulus were comparable. The entire system exhibited viscous flow macroscopically, as shown in Fig. 9(a) and (b), indicating fewer connections between the molecular chains and resulting in poor mechanical strength and toughness. Fig. 10 shows the stress-strain curves of the polymer gels prepared at gelling temperatures of 120 and 140 °C. As the gelling temperature increased, the thermal motion of the molecular chains intensified, leading to more frequent collisions and entanglements between chains, which in turn resulted in a gradual increase in crosslinking density. The tensile stress prepared at a gelling temperature of 120 °C was 30.07 kPa and the strain was 539.54%. Under external tensile stress, the molecular chains were able to adjust their lengths to maintain network balance and avoid stress concentration. Additionally, the ordered arrangement and dense crosslinking of molecular chains enhanced the gel's toughness and improved its mechanical properties. When the gelling temperature was increased to 140 °C, the tensile stress of the prepared polymer gel decreased from 30.07 to 8.145 kPa, and the strain decreased from 539.54% to 445.11%. This result indicates that a higher gelling temperature does not necessarily yield better mechanical performance. At elevated temperatures, the gel loses water and becomes hard, with increasing gelling temperature, the long molecular chains in the gel struggle to reorganize into an ordered network structure, losing their ability to undergo phase transitions. Moreover, the density and effectiveness of intermolecular crosslinking are significantly reduced, as is the number of effective crosslinking sites per unit volume. As a result, inefficient network structures develop, which do not contribute to the mechanical strength of the gel and ultimately lead to a decline in overall mechanical performance. Jiang et al. (2014) concluded that increasing the synthesis temperature accelerates the movement of water molecules and polymer chains, which weakens the hydrophobic interactions that are critical to the formation and stability of polymer gels. Therefore, the loss of hydrophobicity during gel formation at high temperatures also adversely affects gel performance. These factors demonstrate that the mechanical properties of polymer gels decline significantly as the gelling temperature continues to increase beyond an optimal threshold.

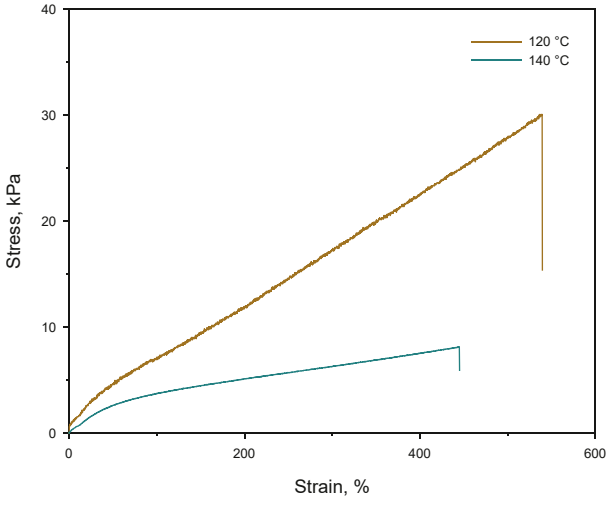

Fig. 10. Relationship between tensile stress and strain of gels formed at different gelling temperatures with a gelling time of 10 h and a concentration of 14%.

6. Effect of gelling time on gel properties

6.1. Effect on rheological mechanical properties

Gelling time directly influences pumping, transporting, and plugging behavior of the gel during lost circulation control and significantly affects its rheological and mechanical properties. As shown in Fig. 11(a), under a gelling temperature of 120 °C, a concentration of 14%, and a strain of $\gamma = 10\%$, when the gelling time was extended from 2 to 8 h, the storage modulus rose from 121 to 320 Pa, while the loss modulus dropped from 202 to 140 Pa. At this time, the polymer gel system exhibited soft and viscous characteristic as shown in Fig. 12(a–c). Its rheological behavior was similar to viscous fluids. Through scanning electron microscopy (Fig. 12(g)), it can be observed that the microstructure surface of the polymer gel at the gelling time of 4 h has a lot of bumps and is relatively rough. Between 8 and 10 h of gelling time, under the strain condition of $\gamma = 10\%$, the storage modulus increased from 320 to 375 Pa, and the loss modulus decreased from 140 to 104 Pa. This change results from the development of a completer and more stable network, as prolonged gelling time allows polymer chains to generate more crosslinking points. At the macroscopic level, a clear transition occurs from a viscous flow state to a highly elastic state (Fig. 12(c) and (d)). This network structure plays a decisive role in the rheological properties of polymer gels, and its rheological behavior gradually approaches that of elastic solids, which make the polymer gel gradually become more ductile, and it can better resist deformation and store energy. Therefore, the storage modulus of the gel increases with the gelling time, while the loss modulus tends to decrease. Sun et al. (2021) also confirmed through their research on the mechanical state transition mechanism of polymer materials. Angular frequency scans were performed on polymer gels with different gelling times at a constant strain $\gamma = 1\%$ (Fig. 11(b)). When the gelling time of the polymer gel increased from 2 to 14 h, its storage modulus ultimately stabilized at around 512 and 1136 Pa, and the loss modulus finally stabilized at around 551 and 476 Pa. However, when the gelling time became excessive, such as 10–14 h, the molecular chains in the polymer gel became more tightly entangled. The microstructure of the gel at 14 h (Fig. 12(g)) gelling time exhibit fewer protrusions and a smoother surface compared to those formed at 12 h (Fig. 12(h)). This structural refinement results from tighter molecular cross-linking induced by prolonged gelation. However, excessive crosslinking may limit chain mobility, leading to reduced rheological performance. In this case, the loss modulus begins to rise again with prolonged gelling time.

6.2. Effect on mechanical properties

Gelling time is a critical parameter in the preparation of polymer gel, as it significantly influences their mechanical properties. For lost circulation control, the plugging material must possess sufficient toughness to withstand downhole mechanical stress. However, gelling time did not exhibit a linear correlation with the mechanical properties of polymer gels (Fig. 13). In the early stage of gel formation, when the gelling time was 2 h, the polymer gel system remained in a dilute solution state as shown in Fig. 12(a), which did not reflect its mechanical properties. When the gelling time was increased from 4 to 10 h, the polymer gel exhibited softer and more deformable characteristics as shown in Fig. 12(b–d).

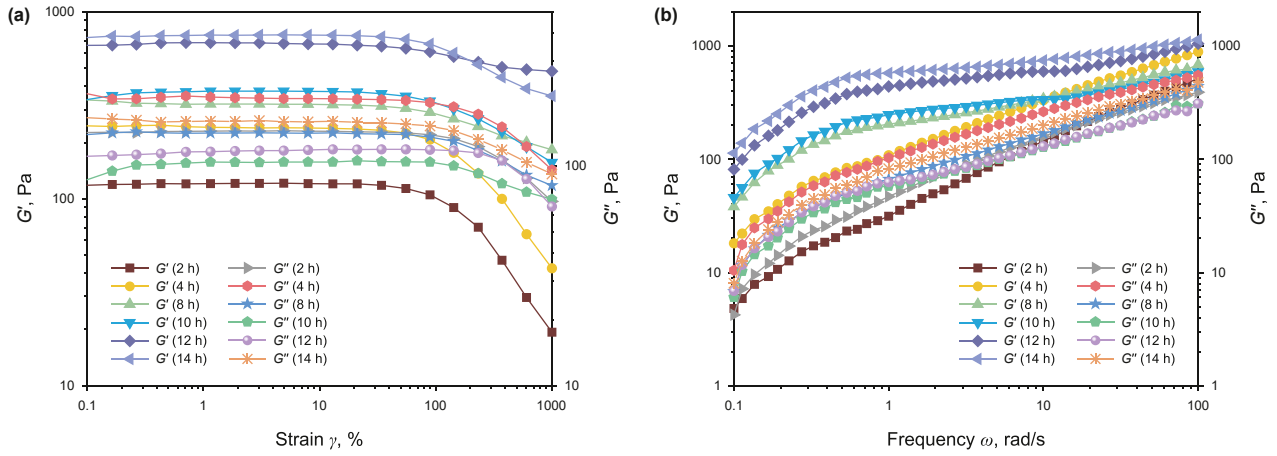

Fig. 11. Gelling temperature 120 °C, 14% concentration: (**a**) relationship between gel strain and modulus at different gelling times; (**b**) relationship between gel angular frequency and modulus at different gelling times.

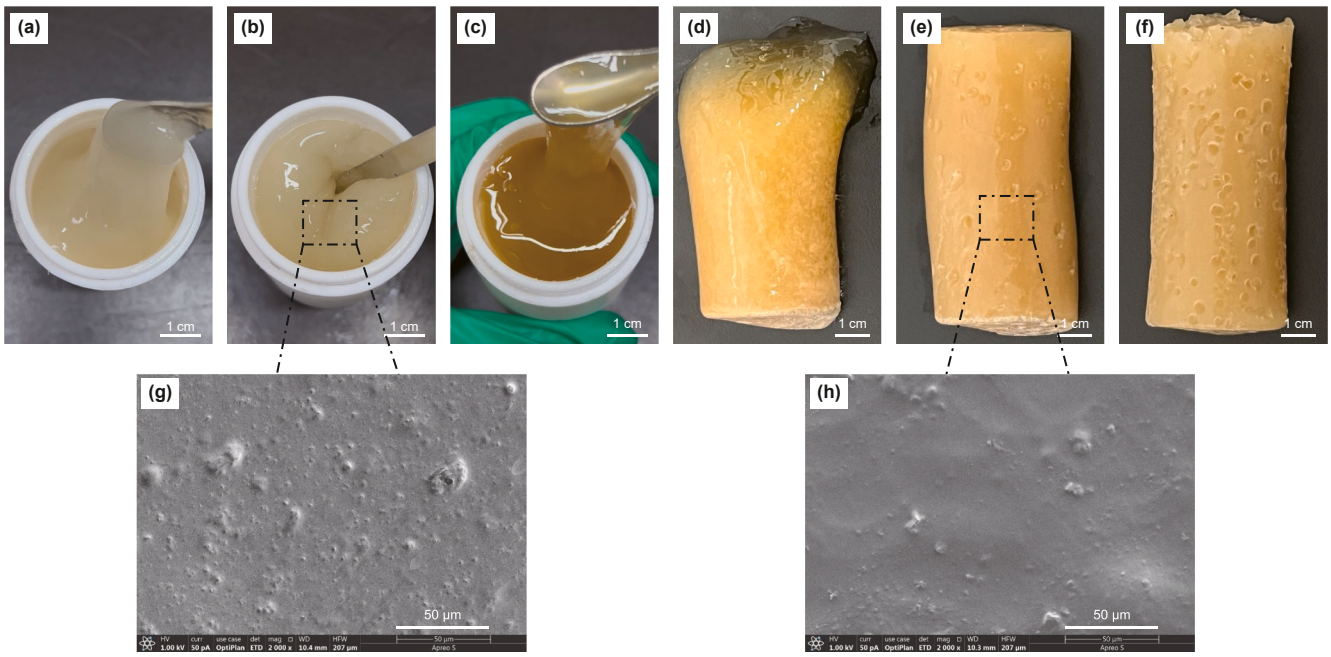

Fig. 12. (**a**–**f**) Physical images of gel formation at a gelling temperature of 120 °C and a concentration of 14% for different gelling times: (**a**) 2 h; (**b**) 4 h; (**c**) 8 h; (**d**) 10 h; (**e**) 12 h; (**f**) 14 h; (**g**, **h**) SEM images of gels formed at 120 °C and 14% concentration for different gelling times: (**g**) 4 h; (**h**) 12 h.

During this period, the tensile stress of the polymer gel increased from 4.103 to 30.07 kPa, while the strain decreased from 532% to 368.63% and then increased to 539.54%. This behavior suggests that within this time range, the extension of gelling time allowed polymer chains to form a more complete and stronger network structure through crosslinking effects, resulting in gradually increased tensile stress. However, after a certain period of time, the gel structure reached a certain saturation point, and further increasing the gelling time did not continue to strengthen the structure but instead led to structural relaxation, resulting in increased strain. When the gelling time was increased from 10 to 12 h, the internal structure of the polymer gel became more compact as the temperature continues to rise, and the density of effective crosslinking points per unit volume dropped significantly. The tensile stress of the gel decreased from 30.07 to 11.33 kPa, and the strain decreased from 539.54% to 493.88%. With the further extension of time to 14 h, the gel network underwent secondary evolution. Through additional crosslinking and structural rearrangement, the overall tensile stress of the gel increased again to 43.91 kPa. However, due to overly dense crosslinking, the molecular chains lost flexibility, making it difficult for deformation and elongation to occur during stretching. As a result, the strain continued to decrease to 374.62%. This nonlinear relationship indicates that the degree of crosslinking varies in a complex manner with gelling time. Therefore, appropriately extending the gelling time enables the preparation of polymer gels with enhanced strength and toughness, thereby improving the mechanical performance of plugging materials for field applications.

7. Long-term stability of gel at high temperature

7.1. Effect on rheological mechanical properties

Polymer gel was aged with a concentration of 14% at 120 °C for 3, 7, 10, 15, 20, and 30 days to evaluate their thermal resistance and

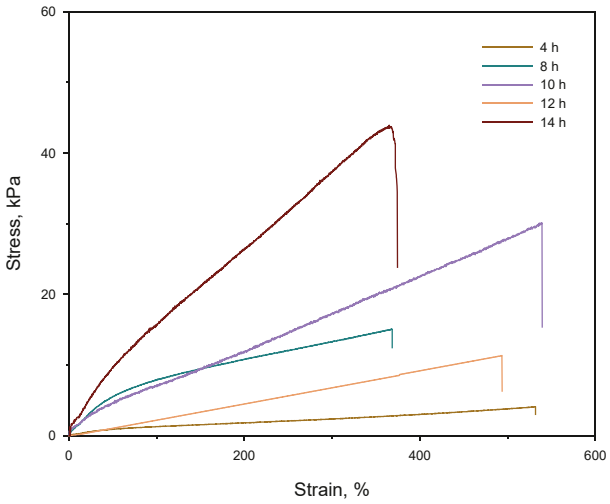

Fig. 13. Relationship between tensile stress and strain of gels with different gelling times at a gelling temperature of 120 °C and a concentration of 14%.

to further assess the structural stability of the gel. The storage modulus and loss modulus of the gel were measured using a rheometer to investigate the influence of aging time on its rheological behavior. As shown in Fig. 14(a), both the storage modulus and loss modulus initially increased and then decreased with the aging time, as the aging time increased from 3 to 7 days, the storage modulus increased from 1651 Pa to a maximum of 1907 Pa. As the aging time was further extended to 30 days, the storage modulus decreased to 1049 Pa; When the aging time was extended from 3 to 10 days, the loss modulus increased from 128 Pa to a maximum of 312 Pa. As the aging time extended to 30 days, the loss modulus decreased to 137 Pa. These changes in the rheological properties of polymer gels had a great relationship with the extension of the aging time to affect the internal crosslinking network structure. During the initial aging stage of 3–7 days, additional crosslinking reactions occurred between molecular chains, forming a denser network structure, which enhanced the gel's storage modulus and structural stability. Fig. 15(h) shows that the scanning electron microscope image of the polymer gel after 7 days of aging exhibits a very dense and smooth structure, with no honeycomb-like pores or depressions. However, as the aging time continued to increase, the molecular chain breakage and degradation occurred (Fig. 15(a)), resulting in a looser internal network with visible depressions (Fig. 15(i)) and a subsequent decline in modulus values. The storage modulus also decreases accordingly. At the same time, with increasing angular frequency, the storage modulus and loss modulus of the polymer gel first rose sharply and then tend to stabilize. When the aging time was extended from 3 to 7 days, the storage modulus finally stabilized at around 1810 and 1888 Pa. When the aging time was extended to 30 days, the storage modulus finally stabilized at 1251 Pa; When the aging time was extended from 3 to 10 days, the loss modulus eventually stabilized at around 358 and 583 Pa. With aging time prolonged to 30 days, the loss modulus eventually stabilized at 456 Pa. Throughout the aging period, the storage modulus consistently exceeds the loss modulus, suggesting that the gel system maintains good mechanical strength and exhibits stable behavior under high-temperature conditions. These results confirm the gel's suitability for long-term applications in deep, high-temperature reservoirs.

7.2. Effect on mechanical properties

To be effective in downhole applications, polymer gels must retain long-term stability under complex pressure and thermal environments. Consistent with the rheological results, the gel's tensile strength shows an initial increase followed by a decline as aging time progresses. As shown in Fig. 16, when the aging time was extended from 3 to 7 days, the tensile stress increased from 29.52 to a maximum of 38.07 kPa. As the aging time was extended to 30 days, the tensile stress gradually decreased to 21.62 kPa, and the strain of the polymer gel also increased from 237.61% to 351.78%, and then decreased to 298.14% as the aging time continued to increase. These trends are attributed to structural changes occurring during the aging process. In the early stages of aging, the gel becomes more plastic, allowing easier deformation and leading to increased strain. Simultaneously, crosslinking between molecular chains intensifies, enhancing mechanical strength. The resulting increase in crosslinking density improves the gel's resistance to stretching and shearing, allowing it to better withstand external stress. However, as aging time continues to increase, the molecular chains gradually break down with the extension of time, resulting in the destruction of the internal structure, leading to the loss of continuity and reduction of mechanical strength. Nevertheless, after aging for 30 days, the polymer gel still maintained a good elastic solid state (Fig. 15(g)),

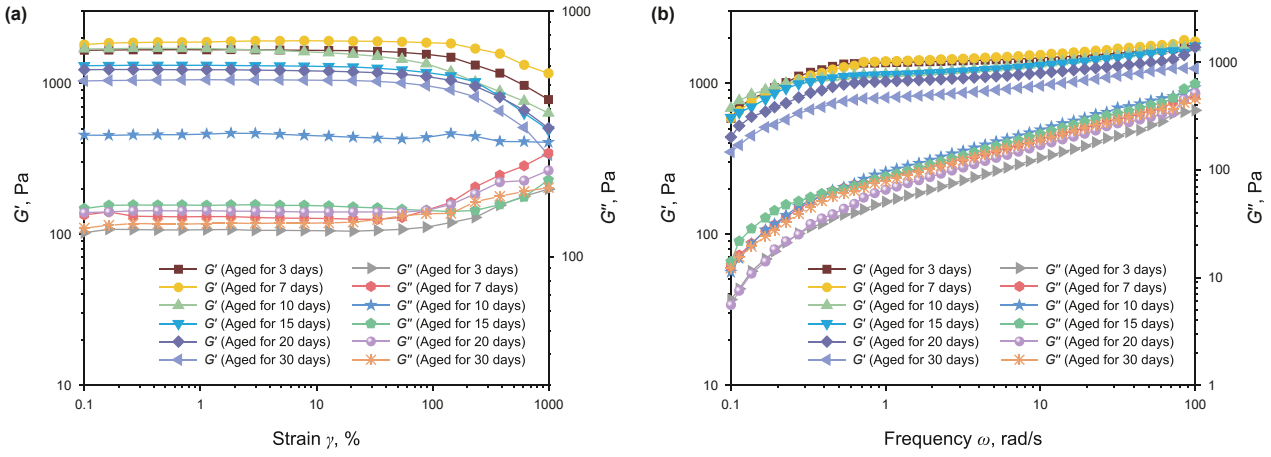

Fig. 14. Gelling temperature at 120 °C, concentration at 14%: (**a**) relationship between strain and modulus of gels with different aging times; (**b**) relationship between angular frequency and modulus of gels with different aging times.

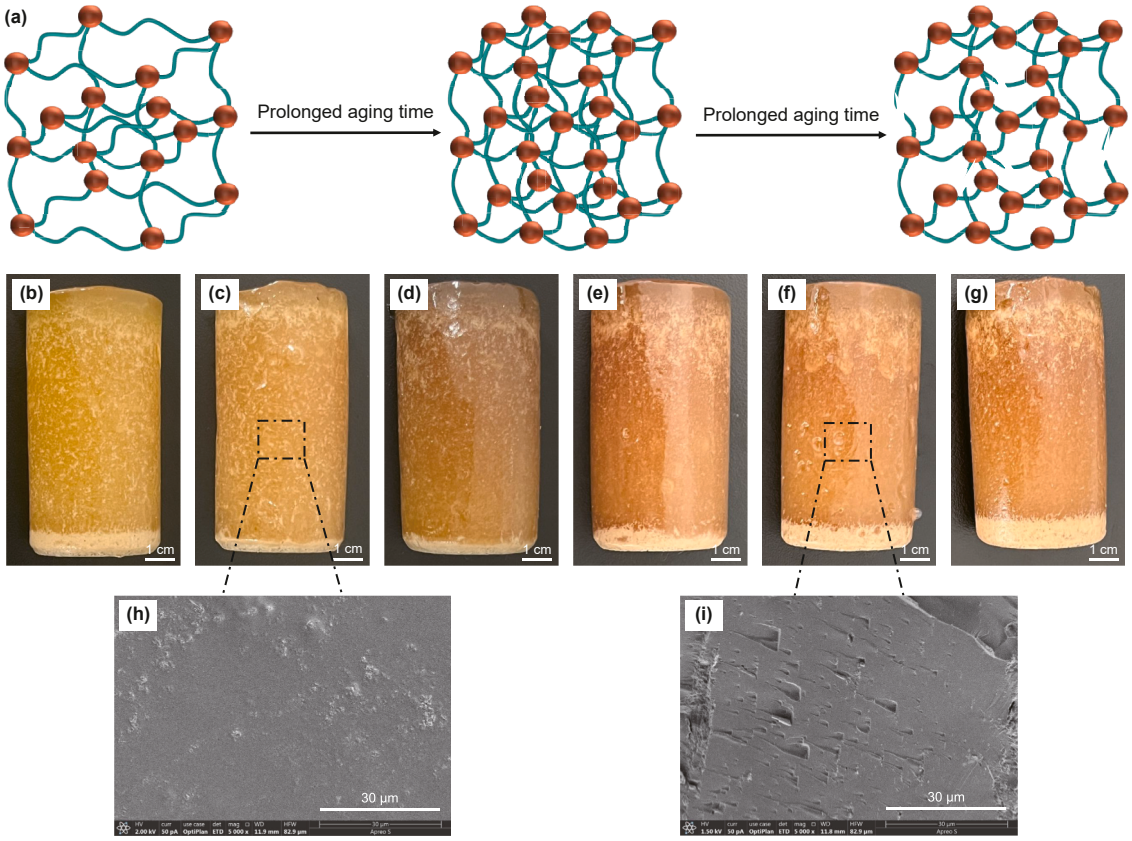

Fig. 15. (**a**) Schematic diagram of the internal network structure of polymer gels with different aging times; (**b**–**g**) physical images of gels with a gelling temperature of 120 °C and a concentration of 14% at different aging times: (**b**) aged for 3 days; (**c**) aged for 7 days; (**d**) aged for 10 days; (**e**) aged for 15 days; (**f**) aged for 20 days; (**g**) aged for 30 days; (**h**–**i**) SEM images of gels with a gelling temperature of 120 °C and a concentration of 14% at different aging times: (**h**) aged for 7 days; (**i**) aged for 20 days.

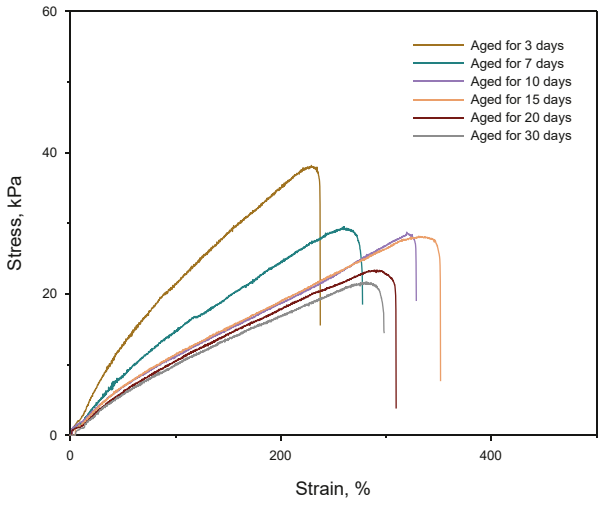

Fig. 16. Relationship between tensile stress and strain of gels with different aging times at a gelling temperature of 120 °C and a concentration of 14%.

compared with that after 3 days of aging, the tensile stress decreased to only 7.9 kPa, while the strain increased by 60.53%. These results clearly demonstrate that the polymer gel system developed in this study exhibits excellent thermal stability and mechanical robustness, making it highly suitable for use in high-temperature, high-pressure reservoir environments.

8. Polymer gel plugging experiment

We synthesized a polymer gel solution and injected it into the high-temperature and high-pressure fracture plugging simulation device to evaluate its pressure-bearing plugging performance in both fractures and sand-filled pipes. The gel was formed under conditions of 14% polymer concentration and a gelling time of 8 h at 140 °C.

In the first experiment, the 14% polymer gel system was injected into a parallel fracture with an inlet and outlet width of 20 mm × 5 mm. After reacting at 140 °C for 8 h, slurry water was injected at a rate of 5 mL/min using an advection pump. As the fluid was injected into the parallel fractures, the fluid pressure in the parallel fractures gradually increased. When the pressure dropped from 5.8 to 4.2 MPa within 2 s after reaching the peak, it indicated that the gel had been damaged under the driving pressure at that point. The maximum breakthrough pressure of the gel was recorded as 5.8 MPa, demonstrating effective plugging performance (Fig. 17(a)). From Fig. 17(b–d), the gel exhibited strong adhesion ability after gelling and was able to effectively fill and plug the inlet and outlet of the fracture.

In the second experiment, the same 14% polymer gel system was injected into a sand-filled pipe with a 3 mm fracture in the inlet and outlet pipelines, an inner diameter of 3 cm, and a length of 20 cm. After reacting for 8 h at 140 °C, the slurry was injected by an advection pump at a water injection rate of 5 mL/min, while the piston pump was used for stepped pressurization. The pressure was first increased to 3 MPa and held static for 10 min to observe pressure stability. Then, the pressure was increased in 2 MPa increments, again with 10-min holding intervals. After reaching

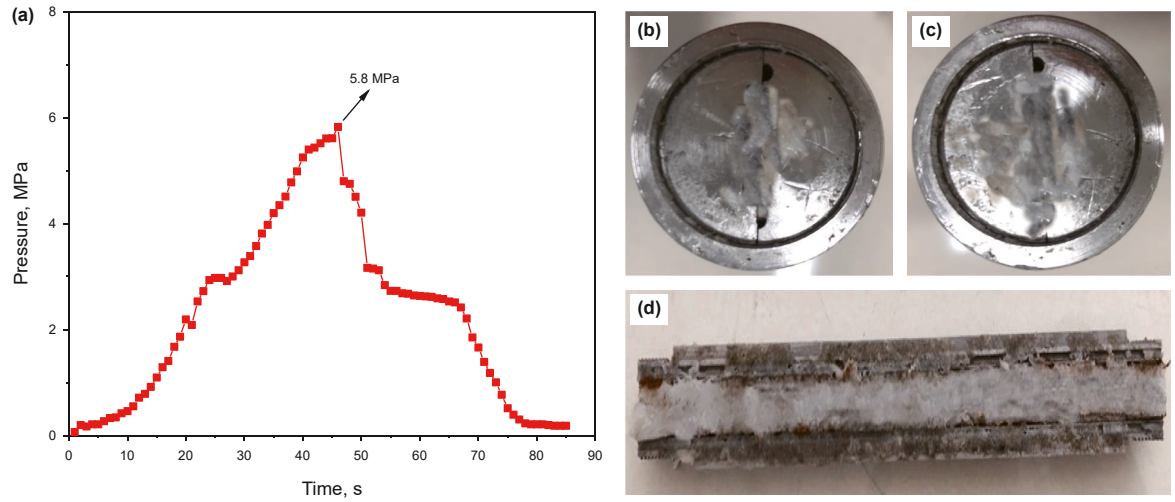

Fig. 17. (**a**) The plugging strength of the gel slug on a parallel fracture with an inlet and outlet size of 20 × 5 mm; (**b–d**) physical images of gel formation in a fracture at a concentration of 14% and a temperature of 140 °C for 8 h: (**b**) the inlet end of the fracture; (**c**) the outlet end of the fracture; (**d**) the gel slug inside the fracture.

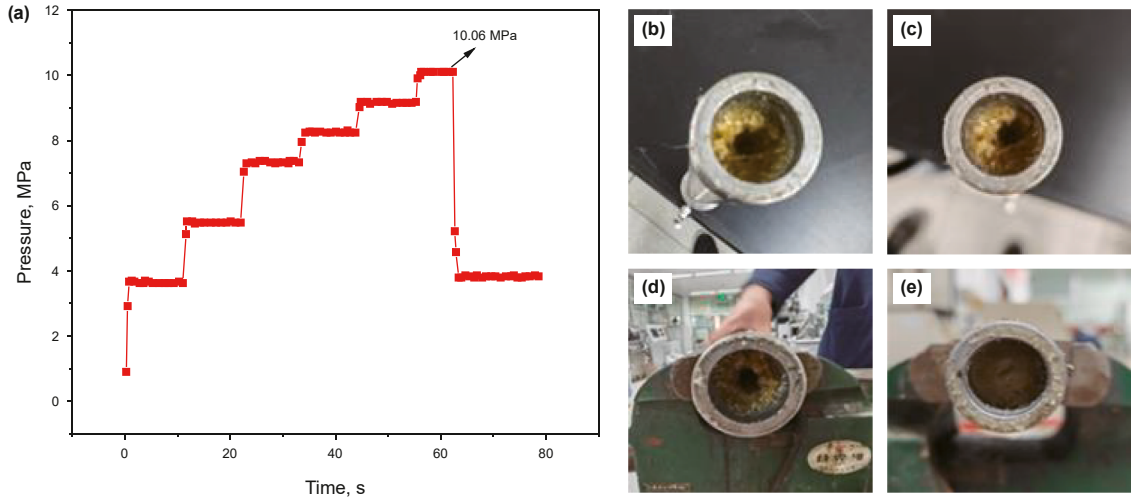

Fig. 18. (**a**) The plugging strength of the gel slug against a sand-filled tube with an inner diameter of 3 cm; (**b–e**) Shows the breakthrough of a gel-filled sand tube with a concentration of 14% and a reaction temperature of 140 °C for 8 h before and after breakthrough: (**b**) before breakthrough at the inlet; (**c**) before breakthrough at the outlet; (**d**) after breakthrough at the inlet; (**e**) after breakthrough at the outlet.

7 MPa, the pressure was increased in 1 MPa increments, with 10-min static intervals at each stage. After the polymer gel applied a pressure of 10.06 MPa to the sand-filled pipe with an inner diameter of 3 cm for 6 min, the polymer gel underwent breakthrough, and 16 mL of the gel mixture was discharged from the outlet (Fig. 18(a)). Compared with the pressure of 8.593 MPa achieved by the wood cellulose hydrogel reported in previous studies conducted in sand-filled pipes (Jiang et al., 2024), these results demonstrated that the polymer gel system possesses strong pressure-bearing capacity and could effectively plug fractures and fracture-vuggy loss formations.

9. Field test of polymer gel plugging

The HD29-H8 well is an exploration well located in the Tarim Basin of Xinjiang, China. Due to the presence of fractures, microfractures, and weak formations, the well is prone to severe loss circulation and other engineering complications during drilling. The geothermal gradient is 2.575 °C per 100 m. When drilling reached a depth of 5440 m, the formation temperature was 140.1 °C. Lost circulation occurred at a displacement of 30 L/s, a pump pressure of 22 MPa, and a loss rate of 10 m^3/h, with a cumulative loss of 30.4 m^3 of drilling fluid at a density of 1.32 g/cm^3. These data did not meet the requirements for safe operations, necessitating immediate plugging measures. Initially, a total of 20 m^3 of plugging slurry was injected into the well twice for downhole plugging, but both times were ineffective.

The polymer gel proposed was subsequently applied to plug the fractured formation and stabilize the wellbore (Fig. 19). As shown in Fig. 19(a–d), the polymer gel plugging slurry prepared on the field successfully formed a high strength gel after gelling at 140 °C for 12 h. According to the actual well conditions of HD29-H8 well (Fig. 19(e) and (f)), it is determined that the loss layer section was identified in the Silurian System from 5440 to 5618 m. We prepared polymer gel plugging slurry using domestic water from the HD29-H8 well site, totaling 51 m^3. In the section of 5440–5618 m loss layer, 49.5 m^3 of polymer gel plugging slurry was pumped first, followed by 47 m^3 of displacement fluid. Then, 2 m^3 of annulus was back-extruded, and the loss rate was reduced to 0 m^3/h after shutting down the wells for 12 h. After polymer gel

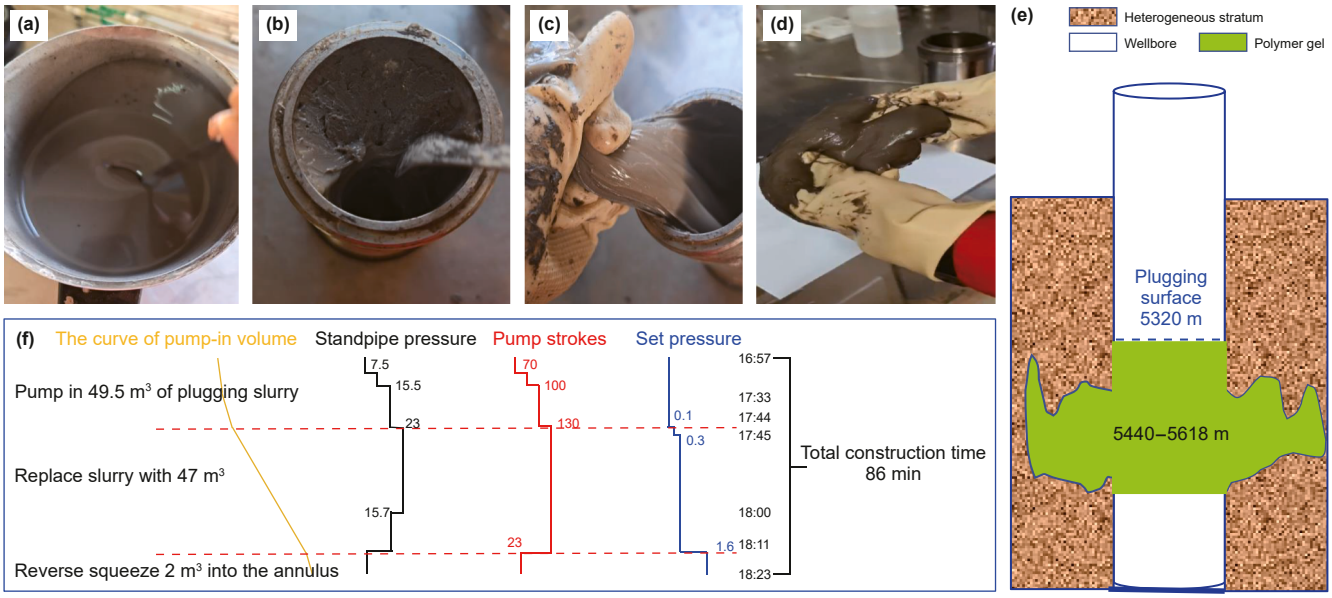

Fig. 19. (**a**–**d**) Polymer gel field slurry preparation; (**e**) polymer gel plugging schematic diagram, (**f**) polymer gel plugging construction curve diagram.

plugging slurry was used to plug the section of 5440–5618 m loss layer, the loss rate did not increase after the plugging gate material was reamed from the gel plugging surface (5320 m) to the well section below 5618 m, indicating that the polymer gel effectively plugged the loss zone. These field results demonstrate that the polymer gel system developed in this study can be effectively applied for plugging fracture formations under high-temperature and high-pressure conditions, providing a reliable solution for lost circulation control in deep and complex reservoirs.

10. Conclusions

In this paper, the effects of different preparation conditions including concentration, gelling temperature, gelling time, and aging time on the rheological and mechanical properties of polymer gels were systematically investigated and analyzed. Combined with microscopic scanning electron microscopy observations, the internal crosslinking mechanism of the gels was elucidated, providing a theoretical basis for optimizing gel formulation to enhance mechanical performance. In addition, this paper investigated the plugging strength of polymer gel on fractures or fracture/vuggy structures through plugging experiments, and fully proved the plugging effect of polymer gel on the formation through field application in the Tarim Oilfield in Xinjiang. The main conclusions are summarized as follows:

(1) Polymer gels with different concentrations were prepared at different gelling temperatures and gelling times using polyacrylamide as the polymerizable, N-methylolacrylamide as the crosslinking agent, urea-formaldehyde resin and silicate fiber as the toughening agent, lithium-based bentonite as the flow regulator, tert-butyl hydroperoxide as the initiator.

(2) Under gelling temperature of 120 °C and gelling time of 10 h, the mechanical properties of the polymer gel significantly improved as the concentration increased from 12% to 20%. The gel formed under high concentration conditions had a storage modulus of 3171 Pa and a tensile stress of 67.8 kPa. As the concentration increased, the gel became denser macroscopically, and the microstructure showed fewer wrinkles and smoother surfaces. However, excessive concentration could lead to increased brittleness. Therefore, the appropriate adjustment of polymer gel system concentration can be applied to different strength plugging materials.

(3) At the gelling time of 10 h and the concentration of 14%, the gelling temperature was increased from 80 to 140 °C. The optimal gelling temperature was 120 °C, at which the gel exhibited superior rheological and mechanical properties, with a storage modulus of 374 Pa, loss modulus of 103 Pa, and tensile stress of 30.07 kPa. Microstructural analysis showed that low gelling temperature resulted in lower gel crosslinking density, while high temperature formed an ordered and dense structure. However, excessively gelling temperature of 140 °C reduced the number of effective crosslinking points. Therefore, the gelling temperature should be balanced between the polymer chain arrangement and the degree of crosslinking to achieve stability in the process of plugging lost circulation.

(4) Gelling time directly affected the processes of pumping, transportation, and plugging of the gel, and had a significant effect on the rheological mechanical properties. At a gelling temperature of 120 °C and a concentration of 14%, extending the gelling time from 2 to 8 h increased the storage modulus and decreased the loss modulus, indicating the formation of a more complete internal network. However, excessive gelling time of 14 h limited polymer chain mobility, resulting in reduced rheological performance and structural brittleness. Therefore, it is necessary to select an appropriate gelling time to improve the compressive, shear, and tensile properties of the plugging material.

(5) The long-term stability properties of the gel at high temperatures were investigated experimentally. Results showed that during the aging process from 3 to 30 days, the rheological and mechanical properties of polymer gels increased and then decreased. Initially, the gel maintained better elasticity and stable structure, and excessive aging led to the late molecular chain breakage and decrease in gel strength, but the storage modulus remained higher than the loss modulus, and the gel always maintained better elasticity and long-term stability in complex underground environment.

(6) At a concentration of 14% and gelling conditions of 140 °C for 8 h, the polymer gel achieved plugging strength of 5.8 MPa in parallel fracture with an inlet and outlet size of 20 mm × 5 mm, and 10.06 MPa in a sand-filled pipe with a 3 mm fracture, 3 cm inner diameter, and 20 cm length. Field application in Tarim Oilfield in Xinjiang showed that the polymer gel had achieved certain plugging effect for the loss formation. These findings demonstrated that the polymer gel system developed in this study was highly suitable for plugging high-temperature, high-pressure oil and gas reservoirs.

CRediT authorship contribution statement

Yuan Liu: Writing – review & editing, Writing – original draft, Methodology, Investigation, Data curation, Conceptualization. **Ying-Rui Bai:** Writing – review & editing, Writing – original draft, Supervision, Resources, Funding acquisition, Conceptualization. **Jin-Sheng Sun:** Writing – review & editing, Validation, Supervision, Resources, Funding acquisition. **Kai-He Lv:** Writing – review & editing, Supervision, Resources, Funding acquisition. **Jing-Bin Yang:** Writing – original draft, Methodology, Investigation. **Ke-Qing Yang:** Writing – original draft, Data curation, Conceptualization. **You-Ming Lang:** Investigation, Data curation, Conceptualization.

Declaration of competing interest

The authors declare that they have no known competing financial interests or personal relationships that could have appeared to influence the work reported in this paper.

Acknowledgements

This research is financially supported by the National Science and Technology Major Project for New Oil and Gas Exploration and Development (2025ZD1401903), the National Natural Science Foundation of China (Grant 52374023) and Taishan Scholar Young Expert (tsqn202306117).

References

An, M., Lv, Y., Xu, H., et al., 2016. Effect of gel solution concentration on the structure and properties of gel-spun ultrahigh molecular weight polyethylene fibers. Ind. Eng. Chem. Res. 55 (30), 8357–8363. https://doi.org/10.1021/acs.iecr.6b02116.

Azimi Dijvejin, Z., Ghaffarkhah, A., Sadeghnejad, S., et al., 2019. Effect of silica nanoparticle size on the mechanical strength and wellbore plugging performance of SPAM/chromium (III) acetate nanocomposite gels. Polym. J. 51 (7), 693–707. https://doi.org/10.1038/s41428-019-0178-3.

Bai, B., Zhou, J., Yin, M., et al., 2015a. A comprehensive review of polyacrylamide polymer gels for conformance control. Petrol. Explor. Dev. 42, 525–532. https://doi.org/10.1016/s1876-3804(15)30045-8.

Bai, H., Zhang, Z., Huo, Y., et al., 2022. Tetradic double-network physical cross-linking hydrogels with synergistic high stretchable, self-healing, adhesive, and strain-sensitive properties. J. Mater. Sci. Technol. 98, 169–176. https://doi.org/10.1016/j.jmst.2021.05.020.

Bai, Y., Wei, F., Xiong, C., et al., 2015b. Effects of fracture and matrix on propagation behavior and water shut-off performance of a polymer gel. Energy Fuels 29 (9), 5534–5543. https://doi.org/10.1021/acs.energyfuels.5b01381.

Bai, Y., Shang, X., Wang, Z., et al., 2018. Experimental investigation of nanolaponite stabilized nitrogen foam for enhanced oil recovery. Energy Fuels 32 (3), 3163–3175. https://doi.org/10.1021/acs.energyfuels.7b03798.

Bai, Y., Liu, Y., Yang, K., et al., 2023. Application and research prospect of functional polymer gels in oil and gas drilling and development engineering. Gels 9 (5), 413. https://doi.org/10.3390/gels9050413.

Cao, Q., Wang, X., Wu, D., et al., 2017. Controlled crosslinking strategy for formation of hydrogels, microgels and nanogels. Chin. J. Polym. Sci. 36 (1), 8–17. https://doi.org/10.1007/s10118-018-2061-7.

Chen, J., Li, Z., Qiu, Z., et al., 2018. Study on highly acid soluble fibrous lost circulation materials. Drill. Fluid Complet. Fluid 35 (5), 41–45. https://doi.org/10.3969/j.issn.1001-5620.2018.05.008 (in Chinese).

Dai, C., Xu, Z., Wu, Y., et al., 2017. Design and study of a novel thermal-resistant and shear-stable amphoteric polyacrylamide in high-salinity solution. Polymers 9 (7), 296. https://doi.org/10.3390/polym9070296.

Du, X., Feng, S., Lu, H., et al., 2023. Evaluation of supramolecular gel properties and its application in drilling fluid plugging. Processes 11 (9), 2749. https://doi.org/10.3390/pr11092749.

Elahifar, B., Hosseini, E., 2023. Laboratory study of plugging mechanism and seal integrity in fractured formations using a new blend of lost circulation materials. J. Pet. Explor. Prod. Technol. 13 (4), 1197–1234. https://doi.org/10.1007/s13202-023-01607-4.

El Sayed, M.M., 2023. Production of polymer hydrogel composites and their applications. J. Polym. Environ. 31 (7), 2855–2879. https://doi.org/10.1007/s10924-023-02796-z.

Feng, Y., Gray, K.E., 2017. Review of fundamental studies on lost circulation and wellbore strengthening. J. Petrol. Sci. Eng. 152, 511–522. https://doi.org/10.1016/j.petrol.2017.01.052.

Ivan, C.D., Bruton, J.R., Marc, T., et al., 2002. Making a case for rethinking lost circulation treatments in induced fractures. In: SPE Annual Technical Conference and Exhibition. https://doi.org/10.2118/77353-MS.

Jiang, G., 2014. Tensile mechanical properties of hydrophobic association hydrogels: effect of crosslinking method, synthesis temperature, mineral salt and swelling. J. Macromol. Sci. Part A 51 (2), 165–172. https://doi.org/10.1080/10601325.2014.864929.

Jiang, Z.Y., Yang, H., Ji, Z.N., et al., 2024. Lignocellulosic hydrogel for profile control and water plugging in high salt reservoirs. J. Mol. Liq. 401, 124707. https://doi.org/10.1016/j.molliq.2024.124707.

Kumaki, J., 2015. Observation of polymer chain structures in two-dimensional films by atomic force microscopy. Polym. J. 48 (1), 3–14. https://doi.org/10.1038/pj.2015.67.

Kwon, Y.R., Kim, H.C., Kim, J.S., et al., 2023. Semi-IPN superabsorbent polymer based on itaconic acid and polyvinyl alcohol with improved gel strength and salt resistance. Polym. Eng. Sci. 63 (7), 1943–1952. https://doi.org/10.1002/pen.26336.

Liao, H., Liu, Y., Wang, Q., et al., 2018. Structure and properties of porous poly (vinyl alcohol) hydrogel beads prepared through a physical–chemical crosslinking method. J. Appl. Polym. Sci. 135 (26), 46402. https://doi.org/10.1002/app.46402.

Lin, R., Sun, L., 2022. Numerical simulation of the microscopic plugging mechanism and particle flow process of the microsphere system. ACS Omega 7 (50), 46983–46991. https://doi.org/10.1021/acsomega.2c06088.

Lu, X., Sun, Z., Zhou, Y., et al., 2015. Research on configuration of polymer molecular aggregate and its reservoir applicability. J. Dispersion Sci. Technol. 37 (6), 908–917. https://doi.org/10.1080/01932691.2015.1073599.

Ma, X., Kong, S., Li, Z., et al., 2024. Effect of cross-linking density on the rheological behavior of ultra-soft chitosan microgels at the oil-water interface. J. Colloid Interface Sci. 672, 574–588. https://doi.org/10.1016/j.jcis.2024.06.026.

Pu, W., Zhao, S., Wang, S., et al., 2018. Investigation into the migration of polymer microspheres (PMs) in porous media: Implications for profile control and oil displacement. Colloids Surf. A Physicochem. Eng. Asp. 540, 265–275. https://doi.org/10.1016/j.colsurfa.2018.01.018.

Smilek, J., Jarábková, S., Velcer, T., et al., 2019. Compositional and temperature effects on the rheological properties of polyelectrolyte–surfactant hydrogels. Polymers 11 (5), 927. https://doi.org/10.3390/polym11050927.

Son, D., Hwang, H., Fontenot, J.F., et al., 2022. Tailoring physical properties of dual-network acrylamide hydrogel composites by engineering molecular structures of the crosslinking network. ACS Omega 7 (34), 30028–30039. https://doi.org/10.1021/acsomega.2c03031.

Sun, J., Lei, S., Bai, Y., et al., 2021. Mechanical transformation mechanism of polymer materials and its application prospects in the field of drilling fluids. Acta Pet. Sin. 42 (10), 1382–1394. https://doi.org/10.7623/syxb202110012 (in Chinese).

Sun, J., Yang, J., Bai, Y., et al., 2023. Review and prospect of bridging plugging technology in fractured formation. Petrol. Sci. Bullet. 8 (4), 415–431. https://doi.org/10.3969/j.issn.2096-1693.2023.04.032.

Sun, L., Sun, L., Han, Q., et al., 2019. Water plugging performance of preformed particle gel in partially filled fractures. Ind. Eng. Chem. Res. 58 (16), 6778–6784. https://doi.org/10.1021/acs.iecr.9b00128.

Sweatman, R.E., Wang, H.M., Xenakis, H., et al., 2004. Wellbore stabilization increases fracture gradients and controls losses/flows during drilling. In: Abu Dhabi International Conference and Exhibition. https://doi.org/10.2118/88701-MS.

Vargas, G.G., Andrade, R.M., Loureiro, B.V., et al., 2020. Rheological properties of a crosslinking gel based on guar gum for hydraulic fracture of oil wells. J. Braz. Soc. Mech. Sci. Eng. 42 (10), 498. https://doi.org/10.1007/s40430-020-02579-w.

Wang, P., Li, Z., Nie, X., et al., 2012. Anti-dilution properties of a special gel applied to loss circulation control in drilling. Acta Pet. Sin. 33 (4), 697–701. https://doi.org/10.7623/syxb201204024 (in Chinese).

Xie, B., Ma, J., Wang, Y., et al., 2021. Enhanced hydrophobically modified polyacrylamide gel for lost circulation treatment in high temperature drilling. J. Mol. Liq. 325, 115155. https://doi.org/10.1016/j.molliq.2020.115155.

Xiong, C., Shi, Y., Zhou, F., et al., 2018. High efficiency reservoir stimulation based on temporary plugging and diverting for deep reservoirs. Petrol. Explor. Dev. 45 (5), 948–954. https://doi.org/10.1016/s1876-3804(18)30098-3.

Yang, H., Deng, J., Li, R., et al., 2024. Hierarchical α-Ni(OH)$_2$ with tunable by interlayer anion exchange for degradation of hydroxypropyl guar gum synergistic H_2O_2. Sustain. Mater. Technol. 41, e01075. https://doi.org/10.1016/j.susmat.2024.e01075.

Yao, C., Lei, G., Cathles, L.M., et al., 2015. Research and application of micron-size polyacrylamide elastic microspheres (MPEMs) as a smart sweep improvement and profile modification agent. In: SPE Improved Oil Recovery Conference. https://doi.org/10.2118/179531-MS.

Yun, K., 2021. Weak alkali ASP flooding in the second type reservoir in the a Oilfield profile control technology and effect. IOP Conf. Ser. Earth Environ. Sci. 770 (1), 012072. https://doi.org/10.1088/1755-1315/770/1/012072.

Zhang, Y.S., Khademhosseini, A., 2017. Advances in engineering hydrogels. Science 356 (6337). https://doi.org/10.1126/science.aaf3627.

Zhao, K., Khan, H.U., Li, R., et al., 2013. Entanglement of conjugated polymer chains influences molecular self-assembly and carrier transport. Adv. Funct. Mater. 23 (48), 6024–6035. https://doi.org/10.1002/adfm.201301007.

Zhao, S., Pu, W., Wei, B., et al., 2019. A comprehensive investigation of polymer microspheres (PMs) migration in porous media: EOR implication. Fuel 235, 249–258. https://doi.org/10.1016/j.fuel.2018.07.125.

Zhu, W., Zheng, X., 2021. Effective modified xanthan gum fluid loss agent for high-temperature water-based drilling fluid and the filtration control mechanism. ACS Omega 6 (37), 23788–23801. https://doi.org/10.1021/acsomega.1c02617.

Zou, C., Dai, C., Liu, Y., et al., 2023. A novel self-degradable gel (SDG) as liquid temporary plugging agent for high-temperature reservoirs. J. Mol. Liq. 386 (15), 122463. https://doi.org/10.1016/j.molliq.2023.122463.